

Generation of a Dynamic System of Three-Dimensional Tetrahedral Polycatenanes**

Samuel P. Black, Artur R. Stefankiewicz, Maarten M. J. Smulders, Dominik Sattler, Christoph A. Schalley,* Jonathan R. Nitschke,* and Jeremy K. M. Sanders*

Supramolecular chemistry explores the effects of non-covalent interactions on the self-organization of matter.^[1] One strand of supramolecular enquiry has led to the creation of a variety of structurally and topologically nontrivial mechanically interlocked molecules.^[2] In the pursuit of deepening the complexity of such structures we report herein the formation of a new class of mechanically interlocked molecules in a system of three-dimensional tetrahedral catenanes.

Three distinct reversible processes were used in parallel to enable the creation of metal–organic tetrahedral polycatenanes, namely imine bond formation,^[2a,3] metal–ligand coordination,^[4] and donor–acceptor interactions.^[5] A tetrahedral cage M_4L_6 (A; Scheme 1)^[6] was prepared through the reaction of a suspension (owing to poor solubility) of NDI diamine (6 equiv) with 2-formylpyridine (12 equiv) and iron(II) bis-(trifluoromethane)sulfonimide (4 equiv) in acetonitrile.^[7]

This discrete metallosupramolecular architecture, capable of reversible catenation with an organic macrocycle, was designed to provide a pathway to polycatenated species.^[8] NDI moieties have been widely used in the self-assembly of mechanically interlocked molecules because of their planar, electron-poor aromatic surfaces, which engender favorable aromatic donor–acceptor interactions.^[9] A dynamic combinatorial library^[10] (DCL) of polycatenated cages was thus formed by allowing equilibration of the coordinatively dynamic M_4L_6 tetrahedral cage in the presence of an excess of bis-1,5-(dinaphtho)-[38]crown-10 (B; Scheme 1). ¹H NMR analysis of equilibrated DCLs revealed the binding of B to the cage to be best described by a non-cooperative model,^[11] yielding a crown ether to cage-incorporated NDI binding constant of $794 \pm 34 \text{ L mol}^{-1}$. Controlling crown ether and cage concentrations was found to determine the constitution

of the library, and allowed the preparation of the fully-saturated tetrahedral [7]catenane.^[12]

The ¹H NMR spectrum of cage A (Figure 1b) is consistent with the presence of a mixture of diastereomers with T , S_4 , and C_3 point symmetries in solution, as has been previously observed for analogous cages.^[13] The superposition of diastereomer ¹H resonances lead to broadened and overlapping signals, giving the overall appearance of a T -symmetric complex. The expected M_4L_6 type structure was confirmed by ESI-MS, COSY, and NOESY NMR spectroscopy (see Supporting Information).

For A to be catenated by B, we hypothesized a de-coordination–threading–re-coordination mechanism to occur at the pyridylimine metal chelate linkages (Supporting Information, Figure S11). An analogous mechanism is thought to operate in similar supramolecular hosts during the encapsulation of guests with larger radii than the hosts' pores.^[14]

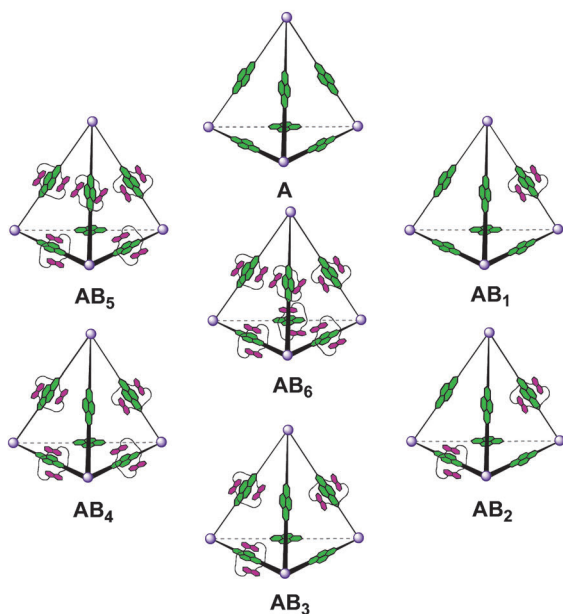
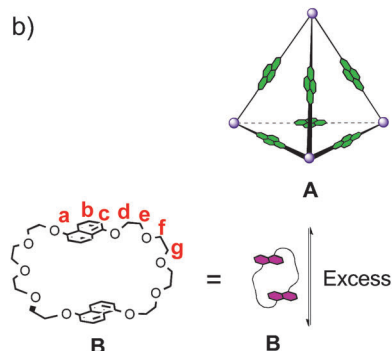
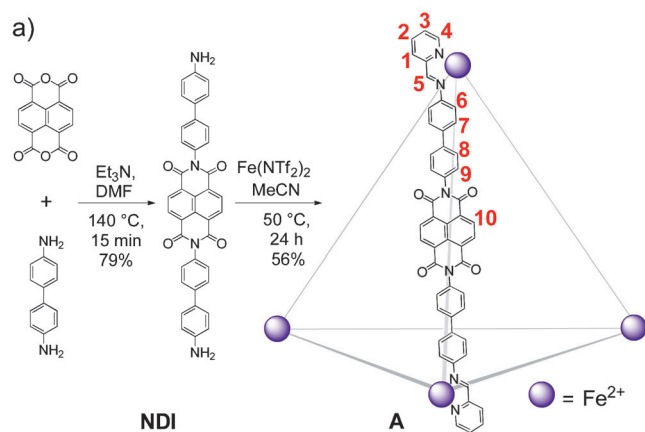
To investigate cage/crown ether binding, an excess of B (10 equiv) was allowed to equilibrate with A (1 equiv, Figure 1c); a minimum of 12 h was found necessary for equilibration (see the Supporting Information). Crown ether signals corresponding to catenation around an NDI axle of cage A were observed. The exchange between free and bound crown ether was observed to be slow on the NMR timescale at 298 K as peaks for the catenated complexes appeared as new resonances and did not shift with changes in crown ether concentration. The ¹H resonances of bound crown ether molecules (Figure 1c, peaks H^a , H^b , and H^c) appeared upfield of resonances attributed to free crown ether (peaks H^a , H^b , and H^c) owing to the close proximity of the shielding aromatic NDI.^[15] We attribute the broadening of the ¹H resonances of cage A in the DCL to loss of symmetry, with the exception of the new NDI peak (peak H^{10} in Figure 1c). The NDI resonance (H^{10}), a singlet at 8.76 ppm in A, split into two signals in the DCL, one encompassing all free NDI binding sites (H^{10*}) at 8.70 ppm and one assigned to all crown ether-bound NDIs (H^{10}), the latter signal being shifted significantly upfield at 8.22 ppm. This peak was integrated relative to the resonances H^a , H^b , and H^c of bound crown ether to confirm the expected one-to-one stoichiometry. Variable-temperature ¹H NMR experiments on the DCL showed only small changes to line shapes and resonance shifts; however, specific catenated species and topological isomers of AB_2 , AB_3 , and AB_4 remained indistinguishable. In an attempt to drive the DCL to the fully saturated [7]catenane, AB_6 , the maximum amount of B soluble in $CD_3CN/CDCl_3$ 1:1 v/v, (38 equiv) was added to A and the mixture was allowed to equilibrate. ¹H NMR spectroscopy (Figure 1d) showed that all NDIs of

[*] S. P. Black, Dr. A. R. Stefankiewicz, Dr. M. M. J. Smulders, Dr. J. R. Nitschke, Prof. J. K. M. Sanders
University of Cambridge, Department of Chemistry
Lensfield Road, Cambridge CB2 1EW (UK)
E-mail: jrn34@cam.ac.uk
jkms@cam.ac.uk
Homepage: <http://www.jrn.ch.cam.ac.uk>

D. Sattler, Prof. C. A. Schalley
Institut für Chemie und Biochemie, Freie Universität Berlin
Takustrasse 3, 14195 Berlin (Germany)
E-mail: christoph@schalley-lab.de

[**] This work was supported by the EPSRC (S.P.B. and J.R.N.), the Netherlands Organization for Scientific Research, NWO (M.M.J.S.), the Deutsche Forschungsgemeinschaft (CRC 765) (D.S. and C.A.S.), and the DSTL (A.R.S. and J.K.M.S.).

Supporting information for this article is available on the WWW under <http://dx.doi.org/10.1002/ange.201209708>.



Scheme 1. a) Synthesis of tetrahedral cage A; b) representation of a DCL formed upon addition of excess crown ether B.

cage A were threaded through a crown ether, and that the library had only a single member, the saturated [7]catenane AB₆.

NOESY analysis was consistent with the expected catenated motif, showing close contact between the bound NDI resonance and the bound macrocycle resonances. Diffusion-ordered spectroscopy (DOSY) was used to examine the

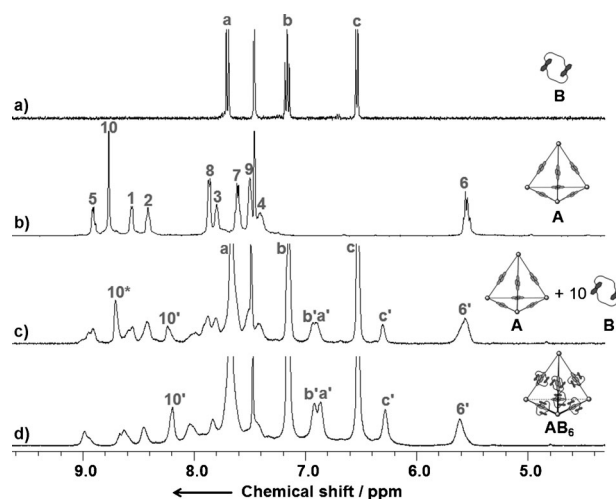


Figure 1. Partial ^1H NMR spectra (400 MHz, $\text{CD}_3\text{CN}/\text{CDCl}_3$ 1:1 v/v, 298 K) of a) crown ether B, b) cage A, c) a DCL formed following the mixture of A (5.4×10^{-4} M, 1 equiv) and B (10 equiv) after 12 h, and d) the [7]catenane obtained by the addition of B (38 equiv) to A (1 equiv) after 12 h. Signals H^a , H^b , and H^c are from crown ether protons threaded around an NDI, and peak H^{10} is the corresponding catenated NDI proton. Peak H^{10*} corresponds to a noncatenated NDI edge of a cage. All other protons are assigned as indicated in Scheme 1.

constitution of a DCL made with 10 equivalents of B. The ^1H DOSY clearly distinguished two crown ether environments (Figure 2). Peaks corresponding to free crown ether B were observed at a diffusion coefficient of $\log D = -9.1$, while all other resonances were observed at a coefficient of $\log D = -9.6$. This second group of resonances includes peaks corresponding to all cage resonances as well as all of the resonances attributed to bound crown ether B. This observation highlights the tight binding between crown ether and cage, as would be expected in catenated structures. Despite the approximate 50% range in mass between catenated DCL constituents, polycatenation leads to an insufficient increase in radii to facilitate their separation in the diffusion dimension. Using the Stokes–Einstein equation,^[16] the above diffusion coefficients correspond to hydrodynamic radii of

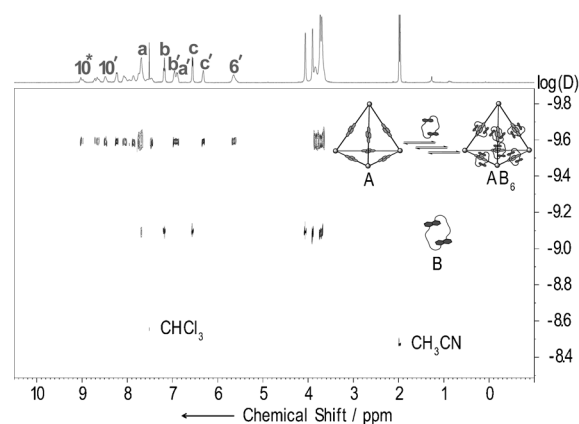


Figure 2. DOSY spectrum (500 MHz, CD₃CN/CDCl₃ 1:1 v/v, 298 K) of a 1:10 cage/crown ether mixture.

6.2 Å and 19.7 Å for the free crown ether and the cage-crown ether adducts, respectively, which is in good agreement with the calculated radii (based on molecular-mechanics-minimized structures) of 7.4 Å and 23 Å respectively (see the Supporting Information). In a control experiment, 10 equivalents of an acyclic congener of B, 1,5-bis[2-(2-hydroxyethoxy)ethoxy]naphthalene, were added to the cage under identical conditions to crown ether/cage DCL formation. No interaction with A could be observed by ^1H NMR spectroscopy (see the Supporting Information for all experimental and analytical details of polycatenane DCL experiments and the control study).

The electrospray Fourier-transform ion-cyclotron-resonance (ESI-FTICR) mass spectrum of A (Figure 3a) exhibited a signal at m/z 612 for the intact cage in its 8+ charge state. Isotope pattern analysis revealed a superposition with an $[\text{M}_2\text{L}_3]^{4+}$ fragment (peak spacing of 1/4 amu) which grew in at the expense of the $[\text{M}_4\text{L}_6]^{8+}$ parent ion (peak spacing of 1/8 amu) in an infrared multiphoton dissociation (IRMPD) tandem MS experiment (Figure 3a, insets), in which the mass-selected parent ion was irradiated with a CO_2 laser at 10.6 μm wavelength. This dissociation was driven by charge repulsion and distributed the charges of the parent ion evenly over two fragments of identical size.^[17] After equilibration of A in the presence of B (1:10 ratio, respectively), the mass spectrum exhibited signals for the expected adducts $[\text{M}_4\text{L}_6\text{C}_n]^{8+}$ ($n = 0-6$ and where C = catenated crown ether), which were superimposed upon the corresponding $[\text{M}_2\text{L}_4\text{C}_{n/2}]^{4+}$ ions for even values of n . Adducts carrying seven or eight crown ethers were also observed, indicating that unspecific binding can occur in the gas phase. Measurements of the control experi-

ments with cage A and the acyclic naphthalene congener of B further confirmed non-specific binding to be possible in the gas phase, whereas no complexes between these two compounds were observed in solution. These observations raised questions as to whether the $[\text{M}_4\text{L}_6\text{C}_n]^{8+}$ adducts with $n \leq 6$ necessarily involve catenation, or whether these adducts could also result from nonspecific binding.

Confirmation of the specific formation of catenated complexes for $[\text{M}_4\text{L}_6\text{C}_n]^{8+}$ with $n = 1-6$ came from IRMPD experiments. The fragmentation pathways for $[\text{M}_4\text{L}_6\text{C}_6]^{8+}$ are indicated by the arrows in Figure 3c. $[\text{M}_4\text{L}_6\text{C}_6]^{8+}$ fragmented preferentially into two identical $[\text{M}_2\text{L}_3\text{C}_3]^{4+}$ fragments, which further decomposed by crown ether losses and the formation of $[\text{ML}_2]^{2+}$ and $[\text{MLC}]^{2+}$. Competing with this fragmentation was the loss of one crown ether to yield $[\text{M}_4\text{L}_6\text{C}_5]^{8+}$. In contrast, the dissociation of $[\text{M}_4\text{L}_6\text{C}_7]^{8+}$ into the analogous $[\text{M}_2\text{L}_3\text{C}_3]^{4+}$ and $[\text{M}_2\text{L}_3\text{C}_4]^{4+}$ fragments was not observed, the latter of which would appear at an m/z higher than that of the parent ion (Figure 3d). Instead, the loss of the non-specifically bound crown ether was the only initial reaction of $[\text{M}_4\text{L}_6\text{C}_7]^{8+}$, which formed $[\text{M}_4\text{L}_6\text{C}_6]^{8+}$, the consecutive fragmentation of which explained all other fragments seen in the IRMPD spectrum of $[\text{M}_4\text{L}_6\text{C}_7]^{8+}$. This observation indicated that the crown ether loss from $[\text{M}_4\text{L}_6\text{C}_7]^{8+}$ occurred at significantly lower internal energies than that from $[\text{M}_4\text{L}_6\text{C}_6]^{8+}$. It can be concluded from this analysis that the seventh crown ether is non-specifically bound in $[\text{M}_4\text{L}_6\text{C}_7]^{8+}$ and that the major fraction of the $[\text{M}_4\text{L}_6\text{C}_6]^{8+}$ ions have an intact tetrahedral structure with all six crown ether molecules threaded.

^1H NMR spectroscopy was used to monitor speciation at increasing concentrations of crown ether B. As no one species of (poly)catenated cage could be distinguished (and thus quantified) owing to the overlap of signals, only information about the average degree of catenation could be obtained.

The fraction of bound NDI was calculated for several equilibrated samples with increasing crown ether concentration and plotted against crown ether concentration (Figure 4; for spectra, see the Supporting Information, Figure S26). The obtained binding isotherm fitted well to a one-to-one binding model, which assumes no cooperativity between the possible six binding events per cage. Our rationalization for this non-cooperative behavior is that cage A is spacious enough for the threading of 6 crown ether molecules, with little steric hindrance between bound crown ether molecules. This hypothesis was validated by geometrical information obtained from a molecular model of AB_6 (see Supporting Information). An intrinsic binding constant for the NDI-crown ether interaction $K_{\text{chem}} = 794 \pm 34 \text{ L mol}^{-1}$ was thus determined and found to be consistent with reported studies.^[18]

Assuming non-cooperative behavior, binding constants for the individual binding events of six consecutive crown ether molecules on to one cage could be calculated, taking into account the statistical factors.^[19] On the basis of these values it was possible to calculate and plot the fraction of each of the different AB_x adducts as a function of crown ether concentration (Figure 4). To test the validity of our assumption of non-cooperativity, we calculated how the degree of

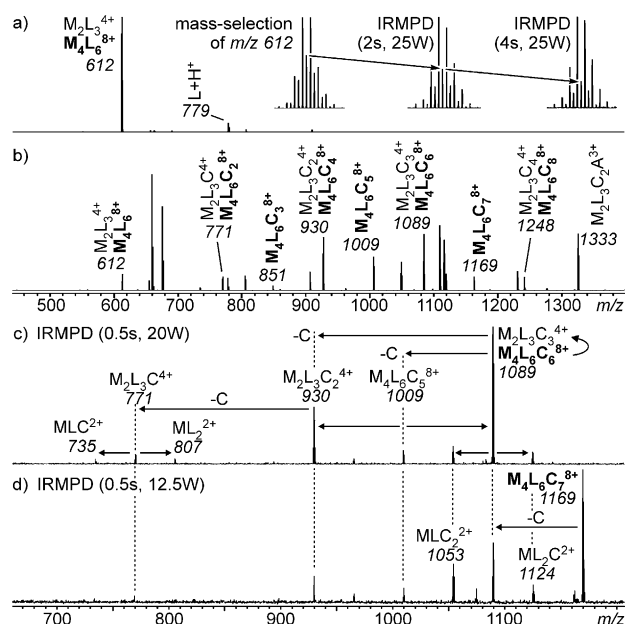


Figure 3. Electrospray Fourier-transform ion-cyclotron-resonance mass spectrometry. a) ESI-FTICR mass spectrum of A. Insets show isotope patterns after mass-selection at different time intervals of irradiation in an IR multiphoton dissociation experiment. b) ESI-FTICR mass spectrum of a 1:10 cage/crown ether mixture. c), d) spectra obtained from IRMPD experiments performed with mass-selected $[\text{M}_4\text{L}_6\text{C}_6]^{8+}$ and $[\text{M}_4\text{L}_6\text{C}_7]^{8+}$ ions, respectively.

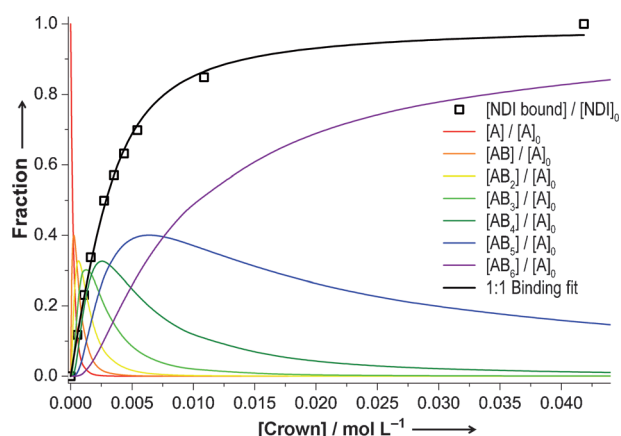


Figure 4. Binding isotherm showing the fraction of bound NDI, $[NDI \text{ bound}]/[NDI]_0$, versus the total concentration of B, $[Crown B]$, as derived from 1H NMR equilibrium data. Squares represent the experimental data points (for full details of NMR analysis and data treatment, see the Supporting Information, Section S8). The black trace is the fitting of the data using a one-to-one binding model, yielding $K_{chem} = 794 \pm 34 \text{ L mol}^{-1}$. Colored lines represent the calculated composition of the intermediate cage/crown ether complexes as a function of crown ether concentration.

NDI binding (as a function of crown ether concentration) changed when putative anti-cooperative effects were included. It was found that the addition of anti-cooperative effects led to a departure of the best fit line from the data points (Supporting Information, Figure S28). Because the observation of a non-cooperative mechanism for catenation was determined by measuring only the NDI-crown ether association, this analysis method cannot fully describe any potential weakening of the iron–ligand binding strength, which might be the outcome of steric clashes within highly catenated species. However, as all of the catenated tetrahedra were observable under identical ESI-MS ionization conditions, we conclude that any such potential weakening is either negligible or non-existent.

In conclusion, we demonstrate that three reversible interactions could be used in concert to create a new class of discrete three-dimensional catenanes, up to and including a complex tetrahedral [7]catenane. Furthermore, this work also shows that full characterization of such complex dynamic systems is possible by bringing to bear a diverse array of analytical techniques. Studies exploring the use of catenation as a mechanism to dynamically block guest ingress and egress to the cavity of related molecular containers are underway.

Received: December 4, 2012
Published online: April 18, 2013

Keywords: catenanes · coordination chemistry · donor–acceptor compounds · mechanically interlocked molecules · supramolecular chemistry

- [1] J.-M. Lehn, *Science* **1993**, *260*, 1762–1763.
[2] a) K. S. Chichak, S. J. Cantrill, A. R. Pease, S.-H. Chiu, G. W. V. Cave, J. L. Atwood, J. F. Stoddart, *Science* **2004**, *304*, 1308–1312;

- b) J.-F. Ayme, J. E. Beves, D. A. Leigh, R. T. McBurney, K. Rissanen, D. Schultz, *Nat. Chem.* **2012**, *4*, 15–20; c) N. Ponnuswamy, F. B. L. Cougnon, J. M. Clough, G. D. Pantoş, J. K. M. Sanders, *Science* **2012**, *338*, 783–785.
[3] a) M. E. Belowich, J. F. Stoddart, *Chem. Soc. Rev.* **2012**, *41*, 2003–2024; b) F. Ibukuro, M. Fujita, K. Yamaguchi, J.-P. Sauvage, *J. Am. Chem. Soc.* **1999**, *121*, 11014–11015; c) D. A. Leigh, P. J. Lusby, S. J. Teat, A. J. Wilson, J. K. Y. Wong, *Angew. Chem.* **2001**, *113*, 1586–1591; *Angew. Chem. Int. Ed.* **2001**, *40*, 1538–1543; d) T. K. Ronson, S. Zarra, S. P. Black, J. R. Nitschke, *Chem. Commun.* **2013**, *49*, 2476–2490; e) S. Zarra, J. K. Clegg, J. R. Nitschke, *Angew. Chem.* **2013**, *125*, 4937–4940; *Angew. Chem. Int. Ed.* **2013**, *52*, 4837–4840.
[4] a) R. Custelcean, J. Bosano, P. V. Bonnesen, V. Kertesz, B. P. Hay, *Angew. Chem.* **2009**, *121*, 4085–4089; *Angew. Chem. Int. Ed.* **2009**, *48*, 4025–4029; b) M. Hutin, C. A. Schalley, G. Bernardinelli, J. R. Nitschke, *Chem. Eur. J.* **2006**, *12*, 4069–4076.
[5] a) M. Fujita, F. Ibukuro, H. Hagihara, K. Ogura, *Nature* **1994**, *367*, 720–723; b) M. A. Alemán García, N. Bampas, *Org. Biomol. Chem.* **2013**, *11*, 27–30.
[6] a) R. W. Saalfrank, A. Stark, K. Peters, H. G. von Schnering, *Angew. Chem.* **1988**, *100*, 878; *Angew. Chem. Int. Ed. Engl.* **1988**, *27*, 851; b) D. L. Caulder, R. E. Powers, T. N. Parac, K. N. Raymond, *Angew. Chem.* **1998**, *110*, 1940–1943; *Angew. Chem. Int. Ed.* **1998**, *37*, 1840–1843.
[7] a) C. O. Dietrich-Buchecker, J. P. Sauvage, J. P. Kintzinger, *Tetrahedron Lett.* **1983**, *24*, 5095–5098; b) P. R. Ashton, T. T. Goodnow, A. E. Kaifer, M. V. Reddington, A. M. Z. Slawin, N. Spencer, J. F. Stoddart, C. Vicent, D. J. Williams, *Angew. Chem.* **1989**, *101*, 1404–1408; *Angew. Chem. Int. Ed. Engl.* **1989**, *28*, 1396–1399; c) E. Wasserman, *J. Am. Chem. Soc.* **1960**, *82*, 4433–4434; d) J. V. Hernandez, E. R. Kay, D. A. Leigh, *Science* **2004**, *306*, 1532–1537.
[8] a) J. E. Beves, B. A. Blight, C. J. Campbell, D. A. Leigh, R. T. McBurney, *Angew. Chem.* **2011**, *123*, 9428–9499; *Angew. Chem. Int. Ed.* **2011**, *50*, 9260–9327; b) H. Deng, M. A. Olson, J. F. Stoddart, O. M. Yaghi, *Nat. Chem.* **2010**, *2*, 439–443.
[9] a) C. R. Martinez, B. L. Iverson, *Chem. Sci.* **2012**, *3*, 2191–2201; b) F. B. L. Cougnon, H. Y. Au-Yeung, G. D. Pantoş, J. K. M. Sanders, *J. Am. Chem. Soc.* **2011**, *133*, 3198–3207.
[10] a) J.-M. Lehn, A. V. Eliseev, *Science* **2001**, *291*, 2331–2332; b) P. T. Corbett, J. Leclaire, L. Vial, K. R. West, J. L. Wietor, J. K. M. Sanders, S. Otto, *Chem. Rev.* **2006**, *106*, 3652–3711; c) S. J. Rowan, S. J. Cantrill, G. R. L. Cousins, J. K. M. Sanders, J. F. Stoddart, *Angew. Chem.* **2002**, *114*, 938–993; *Angew. Chem. Int. Ed.* **2002**, *41*, 898–952.
[11] C. A. Hunter, H. L. Anderson, *Angew. Chem.* **2009**, *121*, 7624–7636; *Angew. Chem. Int. Ed.* **2009**, *48*, 7488–7499.
[12] O. Safarowsky, B. Windisch, A. Mohry, F. Vögtle, *J. Prakt. Chem.* **2000**, *342*, 437–444.
[13] W. Meng, J. K. Clegg, J. D. Thoburn, J. R. Nitschke, *J. Am. Chem. Soc.* **2011**, *133*, 13652–13660.
[14] W. Meng, B. Breiner, K. Rissanen, J. D. Thoburn, J. K. Clegg, J. R. Nitschke, *Angew. Chem.* **2011**, *123*, 3541–3545; *Angew. Chem. Int. Ed.* **2011**, *50*, 3479–3483.
[15] D. G. Hamilton, J. E. Davies, L. Prodi, J. K. M. Sanders, *Chem. Eur. J.* **1998**, *4*, 608–620.
[16] J. T. Edward, *J. Chem. Educ.* **1970**, *47*, 261.
[17] a) B. Brusilowskij, S. Neubacher, C. A. Schalley, *Chem. Commun.* **2009**, 785–787; b) C. A. Schalley, T. Müller, P. Linnartz, M. Witt, M. Schäfer, A. Lutzen, *Chem. Eur. J.* **2002**, *8*, 3538–3551.
[18] M. S. Cubberley, B. L. Iverson, *J. Am. Chem. Soc.* **2001**, *123*, 7560–7563.
[19] G. Ercolani, C. Piguet, M. Borkovec, J. Hamacek, *J. Phys. Chem. B* **2007**, *111*, 12195–12203.